

Article

Separation and Recovery of Rare Earths and Iron from NdFeB Magnet Scraps

Houqing Wang ^{1,2}, Jinliang Wang ^{1,2,*}, Xiang Lei ^{1,2}, Xiaochun Wen ^{2,3}, Dewei Li ^{1,2}, Fupeng Liu ^{1,2}, Wenye Zhou ² and Shengming Xu ^{4,*}

¹ Jiangxi Provincial Key Laboratory of Flash Green Development and Recycling, Jiangxi University of Science and Technology, Ganzhou 341000, China; 7120180013@mail.jxust.edu.cn (H.W.); xianglei108@sina.com (X.L.); lideweisg@163.com (D.L.); fupengliu@126.com (F.L.)

² Faculty of Materials Metallurgy and Chemistry, Jiangxi University of Science and Technology, Ganzhou 341000, China; wulihhz@163.com (X.W.); dz18720113720@163.com (W.Z.)

³ School of Material Science and Engineering, Fujian University of Technology, Fuzhou 350118, China

⁴ Institute of Nuclear and New Energy Technology, Tsinghua University, Beijing 100084, China

* Correspondence: simwjl@163.com (J.W.); smxu@tsinghua.edu.cn (S.X.)

Abstract: NdFeB magnet scraps contain large amounts of iron, which poses challenges in recycling and greatly hinders the recovery of rare earths through direct hydrometallurgical treatment. To address this issue, we conducted tests using a flash furnace to explore the low-temperature reduction behavior of NdFeB magnet scraps under an H₂ atmosphere based on thermodynamic calculations comparing the reduction properties of rare earth oxides (REOs) and iron oxide (FeO_x). The results demonstrated that the reduction rate of FeO_x surpassed 95% under optimal conditions including a reduction temperature of 723 K, a particle size (D₉₀) of 0.45 μm, and an H₂ flow rate of 2 L/min. X-ray diffraction and electron probe microanalysis of the reduction product revealed that the flash reduction at 723 K facilitated the selective reduction of FeO_x, owing to efficient mass and heat transfer. Consequently, a two-step magnetic separation process was employed to separate metallic Fe and REOs from the reduction product. Fe-rich phase, obtained with a remarkable Fe distribution ratio of 90.2%, can serve as an economical raw material for weathering steel. Additionally, the REOs are enriched in REO-rich phase, achieving a distribution ratio of 93.9% and significantly boosting the REO concentration from 30.2 to 82.8 wt%.

Keywords: NdFeB magnet scraps; flash reduction; magnetic separation; rare earths; iron



Citation: Wang, H.; Wang, J.; Lei, X.; Wen, X.; Li, D.; Liu, F.; Zhou, W.; Xu, S. Separation and Recovery of Rare Earths and Iron from NdFeB Magnet Scraps. *Processes* **2023**, *11*, 2895. <https://doi.org/10.3390/pr11102895>

Academic Editors: Inês Portugal, Carlos Manuel Silva and José Aniceto

Received: 6 September 2023

Revised: 24 September 2023

Accepted: 27 September 2023

Published: 30 September 2023



Copyright: © 2023 by the authors. Licensee MDPI, Basel, Switzerland. This article is an open access article distributed under the terms and conditions of the Creative Commons Attribution (CC BY) license (<https://creativecommons.org/licenses/by/4.0/>).

1. Introduction

NdFeB magnetic materials are widely used in various high-technology fields because of their excellent remanence, magnetic energy product, and intrinsic coercivity [1,2]. NdFeB magnet scraps are primarily produced during cutting, grinding, and polishing, accounting for ~30% of raw materials in the production of magnets. According to various reports [3–6], the NdFeB magnet scraps containing ~25% rare earth and ~65% iron, which are considerably higher fractions than those found in natural ores, can thus be considered to constitute a valuable “urban mine”.

Numerous studies have been dedicated to the recycling of NdFeB magnet scraps. Several pyrometallurgical methods, such as the glass slag method [7], selective chlorination [8], and liquid metal extraction [9], have been previously explored for NdFeB recovery. However, these approaches typically involve high energy consumption and result in low yields of rare earths, leading to secondary pollution through exhaust gas and waste residue release. In contrast, hydrometallurgical techniques [10–12] offer distinct advantages, such as high leaching efficiencies and the production of high-purity rare earth oxide (REO) products. Among these, conventional hydrochloric acid leaching followed by extractive separation [6], commonly utilized in industries like Ganzhou YouLi Technology in Ganzhou,

China, and Ji'an XinTai Technology in Ji'an, China, has been widely adopted as a method. Nonetheless, a major drawback is the incomplete recovery of the large amounts of iron present in the scraps, which makes the process cumbersome and leads to the significant generation of secondary solid waste or wastewater. Implementing a low-energy process to address these challenges by separating Fe or enriching REOs before acid leaching could greatly enhance the overall economic and environmental value of the recycling processes.

Consequently, a new process needs to be developed for effective Fe separation, particularly the simultaneous recovery of Fe resources and enrichment of REOs. Directly separating Fe_2O_3 and Nd_2O_3 via magnetic separation is difficult owing to their low-intensity magnetic difference [13,14]. However, metallic Fe and Nd_2O_3 are easily and selectively separated via magnetic separation. Fe_2O_3 is reduced in a fixed-step process [15]. Specifically, when the temperature exceeds 843 K, the path for reducing Fe_2O_3 is $\text{Fe}_2\text{O}_3 \rightarrow \text{Fe}_3\text{O}_4 \rightarrow \text{FeO} \rightarrow \text{Fe}$. When the temperature is below 843 K, the path for reducing Fe_2O_3 is $\text{Fe}_2\text{O}_3 \rightarrow \text{Fe}_3\text{O}_4 \rightarrow \text{Fe}$. Pineau et al. [16,17] investigated the low-temperature reduction of Fe_2O_3 using H_2 and observed wüstite and Fe in the reduction product. Therefore, low-temperature reduction below 843 K is feasible using H_2 . However, a major drawback of this process is that the reduction of iron ores using H_2 results in the formation of compact iron layers that can hinder the reduction rate. To avoid this, we first proposed the flash reduction technique [18,19]. The flash furnace is a new and efficient device that has been developed according to the characteristics of raw materials for reduction, oxidation, pyrolysis, and smelting. This technology, owing to its efficient mass and heat transfer and the core technology of rapid fluidized heating, has been widely applied to copper [20], iron [21], and lead [22]. However, the low-temperature reduction behavior of FeO_x in NdFeB magnet scraps, particularly with efficient mass and heat transfer using a flash furnace, has not been reported thus far.

In this study, FeO_x in NdFeB calcine is directly reduced under the conditions of a H_2 atmosphere and then separated via magnetic separation. The flash reaction process must be comprehensively evaluated to efficiently obtain metallic Fe, especially in a short reaction time. Thermodynamic calculations are initially performed using the data in Lange's handbook of chemistry [22,23] to predict the factors controlling the reduction of REOs or FeO_x . The transformations of the Fe-containing phases are characterized using X-ray diffraction (XRD). The effect of flash reduction, followed by magnetic separation, on the microstructure and composition is studied using electron probe microanalysis (EPMA). The method considered in this study can be used to recycle in addition to significantly improving the concentration of REOs. These Fe-rich phases can be utilized as inexpensive raw materials to produce weathering steel without necessitating additional pretreatments. And the influence of impurity element Fe on the subsequent recovery of REOs can be reduced.

2. Experimental

2.1. Materials and Analysis

NdFeB magnet scraps were provided by Ganzhou YouLi Technology, Ganzhou, China. The main components, phase, and morphology of the NdFeB magnet scraps of particle size (D_{90}) 178 μm were comprehensively characterized via roasting, degreasing, grinding, and oxidizing roasting. The phase of NdFeB calcine was confirmed using XRD (Bruker D8 ADVANCE, Karlsruhe, Germany), as shown in Figure 1a. The NdFeB calcine contains crystalline Fe_2O_3 , Nd_2O_3 , and a small amount of FeNdO_3 , respectively. The specific composition was analyzed using inductively coupled plasma-optical emission spectroscopy (ICP-OES, IRIS Intrepid II XSP, Thermo Electron Co., Waltham, MA, USA). The NdFeB calcine contains 65.5% FeO_x , 30.2% REOs, 1.6% SiO_2 , 0.5% CoO , 0.1% CuO , 0.3% Al_2O_3 , 0.3% CaO , and 1.5% other. The morphologies and compositions of the underflow samples were characterized using scanning electron microscopy–energy dispersive spectroscopy (SEM-EDS, MLA650F, Bruker, Karlsruhe, Germany) and EPMA (EPMA-8050G, Shimadzu, Kyoto, Japan), as shown in Figure 1b,c. The calcined NdFeB exhibits a dense morphology, and the REOs and Fe regions are closely linked.

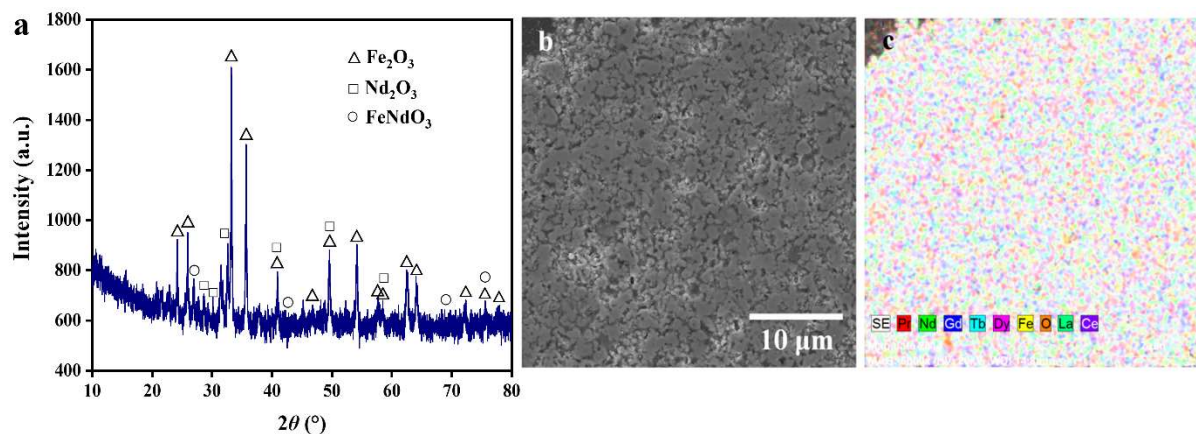


Figure 1. XRD pattern (a) and EMPA analysis (b,c) of the calcined NdFeB.

2.2. Experimental Apparatus and Procedure

Initially, the specific particle size of the material is obtained via high-energy ball milling with a 20:1 ball/materials ratio (FRITSCH P6, Hamburg, Germany), and the particle size analysis is carried out using a laser particle size analyzer (Mastersizer 3000, Malvan, UK). As shown in Figure 2, a flash furnace ($\Phi 127 \text{ mm} \times h 3000 \text{ mm}$), which was fabricated to be custom-made, is used to selectively reduce FeO_x from 100 g of the raw material in several seconds ($\sim 5 \text{ s}$). Because the equipment is a flash furnace and the mass of reaction material is just 100 g, the reduction process is approximately identified as a constant temperature process. The reduction temperature is increased according to the desired heating program, using a mixed gas of H_2 (30%) and N_2 (70%) as the reducing atmosphere. Using the feeding system of the flash furnace, the NdFeB calcine with a carrier gas (N_2 , 0.3 L/min) is sprayed and dispersed into the reaction tower under the combined force of the hot gas flow of the reducing atmosphere, gravity of the sample, and impulse of the carrier gas. The reduction product obtained from the collector is cooled to room temperature and undergoes a two-step wet magnetic separation process. For this purpose, an XCRS-74 magnetic tube (manufactured by Hengshun, Chongqing, China) with varying magnetic field intensities is employed to recover metallic Fe. The first step involves high-intensity ($\geq 100 \text{ mT}$) magnetic separation to achieve a high yield of metallic Fe, while the second step involves low-intensity ($< 100 \text{ mT}$) magnetic separation to attain a high degree of metallic Fe. The resulting magnetic and nonmagnetic products are referred to as metallic Fe (Fe-rich phase) and the REO-rich phase, respectively.

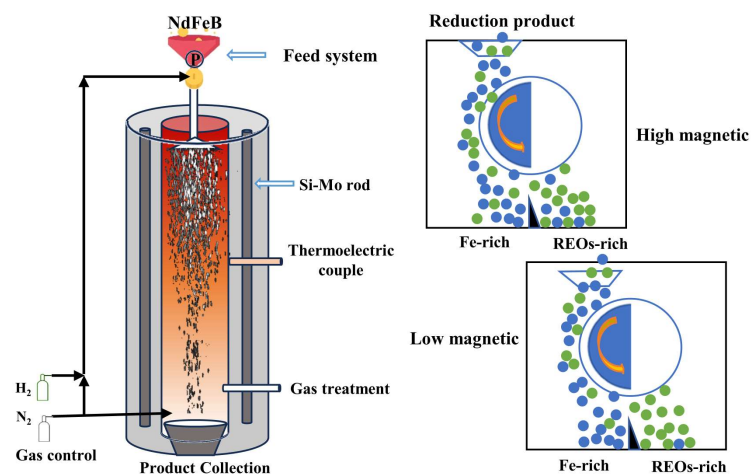


Figure 2. Schematic diagram of the calcined NdFeB produced via flash reduction and magnetic separation.

The reduction rate of FeO_x (η) is calculated using Equation (1):

$$\eta = (m_r/m_c) \times 100\% \quad (1)$$

where m_r is the mass of metallic Fe after reduction (g), and m_c is the total content of Fe in the NdFeB calcine before reduction (g).

The yield of Fe (x) is defined using Equation (2),

$$x = (m_i/m_t) \times 100\% \quad (2)$$

where m_i is the mass (g) of the Fe-rich phase after magnetic separation, and m_t is the total mass (g) of the NdFeB calcine before magnetic separation.

The distribution ratios of Fe (y_f) and REOs (y_e) are then defined using Equations (3) and (4), respectively.

$$y_f = (m_f \times a_f / (m_f \times a_f + m_e \times b_f)) \times 100\% \quad (3)$$

$$y_e = (m_e \times c_e / (m_f \times d_e + m_e \times c_e)) \times 100\% \quad (4)$$

where m_f/m_e is the mass (g) of the Fe-rich/REO phase after magnetic separation; a_f/b_f is the mass fraction of Fe in Fe-rich/REO-rich phase; and d_e/c_e is the mass fraction of REOs in Fe-rich/REO-rich phase.

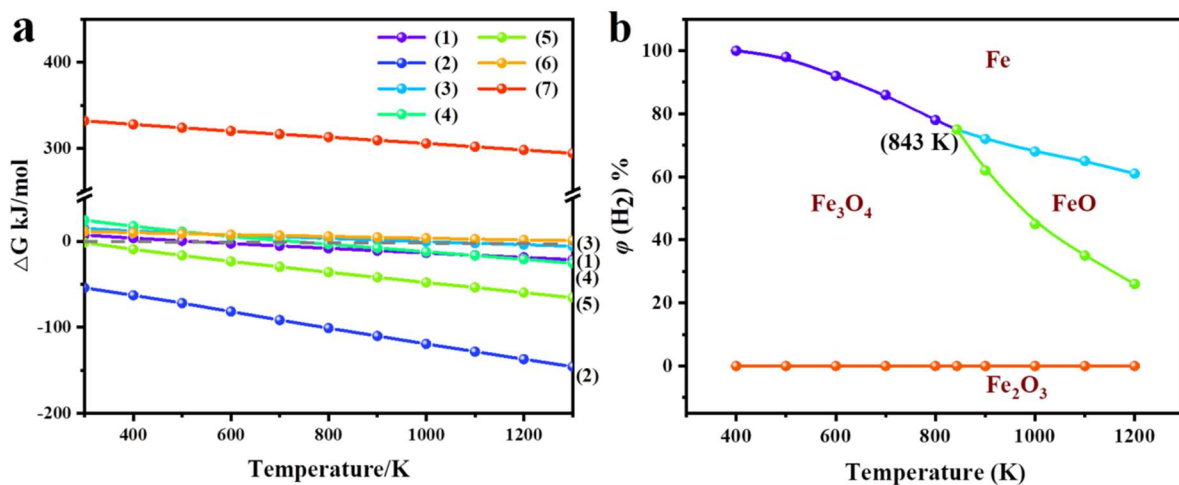
3. Results and Discussion

3.1. Thermodynamic Analysis

The main phases of the NdFeB calcine determined through the raw material source and XRD analysis are listed with the corresponding reduction reaction of flash reduction via H_2 in Table 1. However, thermodynamic data on FeNdO_3 are inadequate due to their low content in terms of the NdFeB calcine; thus, these results are primarily used for the H_2 -based reduction of FeO_x and Nd_2O_3 , the latter representing REOs. Thermodynamic calculations were performed using the data in Lange's handbook of chemistry [23] to predict the factors (such as temperature and reductant concentration) controlling the reduction of rare earths and iron. Lange's handbook of chemistry has the world's favorite and complete thermochemical data. The relationship between temperature (T) and the standard Gibbs free energy change for the reduction reaction is shown in Figure 3. As shown in Figure 3a, H_2 is a good reductant and reacts easily with FeO_x . Moreover, reduction reactions (1–5) can be optimized to facilitate the direct interaction of FeO_x phases with H_2 at lower temperatures (<1000 K). REOs are not to be reduced under the same conditions. Figure 3b displays the compositions of the FeO_x phase under H_2 atmospheric conditions. Based on these results, both the reduction temperature and H_2 concentration are regarded as crucial conditions in this study. Furthermore, Figure 3b reveals that the reduction temperature should be maintained below 843 K. The H_2 concentration should be controlled to exceed 78% to ensure the complete reduction of Fe_2O_3 into metallic Fe. Therefore, the selective reduction of FeO_x could be theoretically achieved according to the thermodynamic calculation. Thereafter, magnetic separation could be used to separate pure Fe and the REO-rich phase.

Table 1. Reactions of the reduction process [23].

Reaction No.	Reactions	ΔG (kJ/mol) vs. T(K)
(1)	$1/3\text{Fe}_2\text{O}_3(\text{s}) + \text{H}_2(\text{g}) = 2/3\text{Fe}(\text{s}) + \text{H}_2\text{O}(\text{g})$	$\Delta G = -0.029T + 15.87$
(2)	$3\text{Fe}_2\text{O}_3(\text{s}) + \text{H}_2(\text{g}) = 2\text{Fe}_3\text{O}_4(\text{s}) + \text{H}_2\text{O}(\text{g})$	$\Delta G = -0.106T - 18.63$
(3)	$\text{Fe}_3\text{O}_4(\text{s}) + 4\text{H}_2(\text{g}) = 3\text{Fe}(\text{s}) + 4\text{H}_2\text{O}(\text{g})$	$\Delta G = -0.019T + 20.19$
(4)	$\text{Fe}_3\text{O}_4(\text{s}) + \text{H}_2(\text{g}) = 3\text{FeO}(\text{s}) + \text{H}_2\text{O}(\text{g})$	$\Delta G = -0.052T + 40.89$
(5)	$\text{Fe}_2\text{O}_3(\text{s}) + \text{H}_2(\text{g}) = 2\text{FeO}(\text{s}) + \text{H}_2\text{O}(\text{g})$	$\Delta G = -0.070T + 21.05$
(6)	$\text{FeO}(\text{s}) + \text{H}_2(\text{g}) = \text{Fe}(\text{s}) + \text{H}_2\text{O}(\text{g})$	$\Delta G = -0.008T + 13.29$
(7)	$1/3\text{Nd}_2\text{O}_3(\text{s}) + \text{H}_2(\text{g}) = 2/3\text{Nd}(\text{s}) + \text{H}_2\text{O}(\text{g})$	$\Delta G = -0.038T + 343.85$

**Figure 3.** The diagram of Gibbs free energy as a function of temperature for Reactions (1–7) (a), equilibrium phase compositions for the H_2 reduction of FeO_x (b).

3.2. Effects of Temperature and Particle Size on the Reduction Rate of FeO_x

Based on the thermodynamic analysis and findings reported in the literature [14,24], the effects of temperature (423, 523, 623, 723, 823, and 923 K) and various particle sizes ($D_{90} = 0.45, 0.87, 3,$ and $37 \mu\text{m}$) on the FeO_x reduction rate were evaluated in this study (Figure 4a). Other initial conditions were fixed, considering H_2 and carrier gas (N_2 gas) flow rates of 2 and 0.3 L/min, respectively. The reaction temperature and particle size considerably influence the reduction efficiencies of FeO_x . When the reduction temperature is increased from 423 to 723 K, the reduction rate of FeO_x increases significantly, particularly in cases of smaller particle sizes (ranging from 5 to 95%). When the temperature exceeds 723 K, the reduction rate of FeO_x with $D_{90} = 0.45 \mu\text{m}$ does not vary significantly, fluctuating around approximately 95%. The smaller particle size, which increases the contact surface of the gas–solid reaction, strengthens the reduction kinetics [25,26]. However, the smaller particle size requires longer durations of grinding and higher levels of energy consumption (Table 2). Considering that the laboratory high-energy ball mill typically cannot be used to grind nanoparticles, $D_{90} = 0.45 \mu\text{m}$ is selected. When the reaction temperature exceeds 723 K and D_{90} is less than $0.45 \mu\text{m}$, the reduction rate of FeO_x approaches 95.2% and tends to stabilize. This result is consistent with the thermodynamic calculations.

Table 2. The particle size of NdFeB calcine obtained by the different grinding time.

Grinding time (h)	4	16	32	56	72
D_{90} (μm)	37	3	0.87	0.45	0.40
D_{50} (μm)	25	2.1	0.58	0.34	0.26
D_{10} (μm)	13	1.2	0.31	0.19	0.14

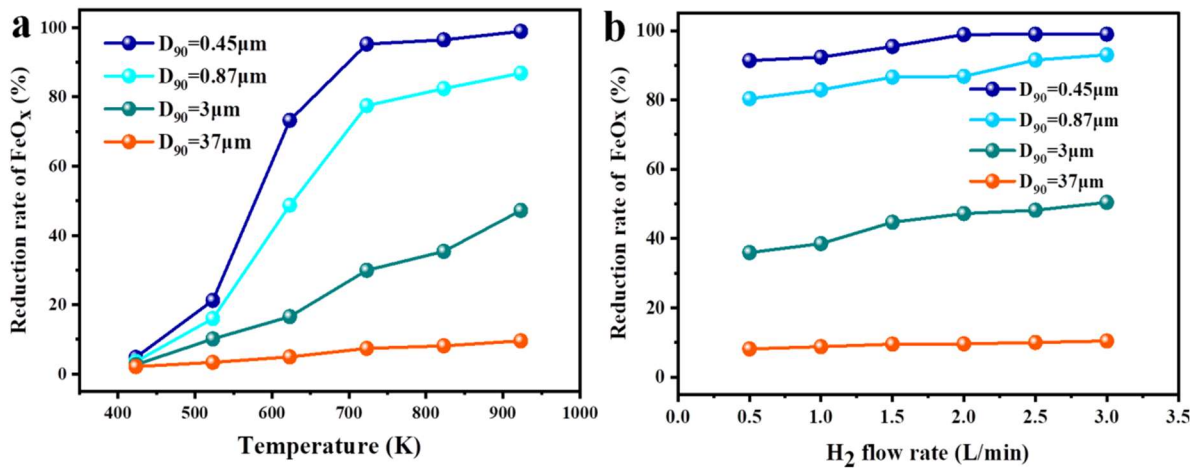


Figure 4. (a) Effect of temperature and particle size on reduction rate of FeO_x (fixed H₂ and N₂ gas flow rates of 2 and 0.3 L/min), (b) effect of H₂ flow rate and particle size on reduction rate of FeO_x (fixed reaction temperature of 723 K and N₂ gas flow rates of 0.3 L/min).

3.3. Effects of H₂ Flow Rate and Particle Size on the Reduction Rate of FeO_x

The effect of H₂ flow rate and particle size on the reduction rate of FeO_x is elucidated in Figure 4b. It is observed that the reduction rate experiences a slight increment as the H₂ flow rate is elevated from 0.5 to 2.0 L/min. However, beyond this point, increasing the H₂ flow rate to 3.0 L/min does not notably affect the reduction rate. Consequently, a H₂ flow rate of 2.0 L/min is deemed optimal. Conversely, the reduction rate exhibits substantial variation at the same H₂ flow rate when particle sizes differ. Remarkably, even in a low reducing atmosphere of 0.5 L/min, a reduction rate of 90% can be achieved. To attain this, a reduction in powder particle size is imperative, thus leading to the selection of a D₉₀ value of 0.45 μm.

To assess the separation of REOs/Fe through magnetic separation, the reduction products undergo characterization using XRD and EPMA (Figures 5 and 6). XRD patterns reveal distinct characteristic peaks corresponding to metallic Fe and Nd₂O₃, providing further confirmation of the selective reduction of Fe through flash reduction. EPMA results further substantiate this, indicating an enrichment of Fe and REOs, with massive Fe₂O₃ particles reduced into elliptic metallic Fe particles. This effective separation of Fe and rare earth within reduction products facilitates the subsequent magnetic separation of Fe and REOs, a crucial step in the process.

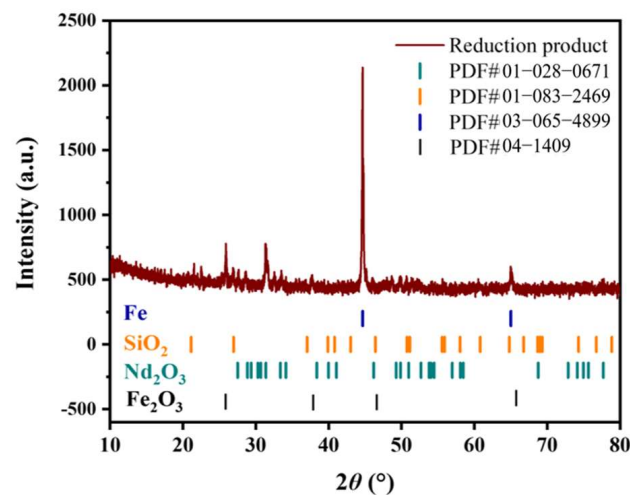


Figure 5. XRD pattern of the reduction product.

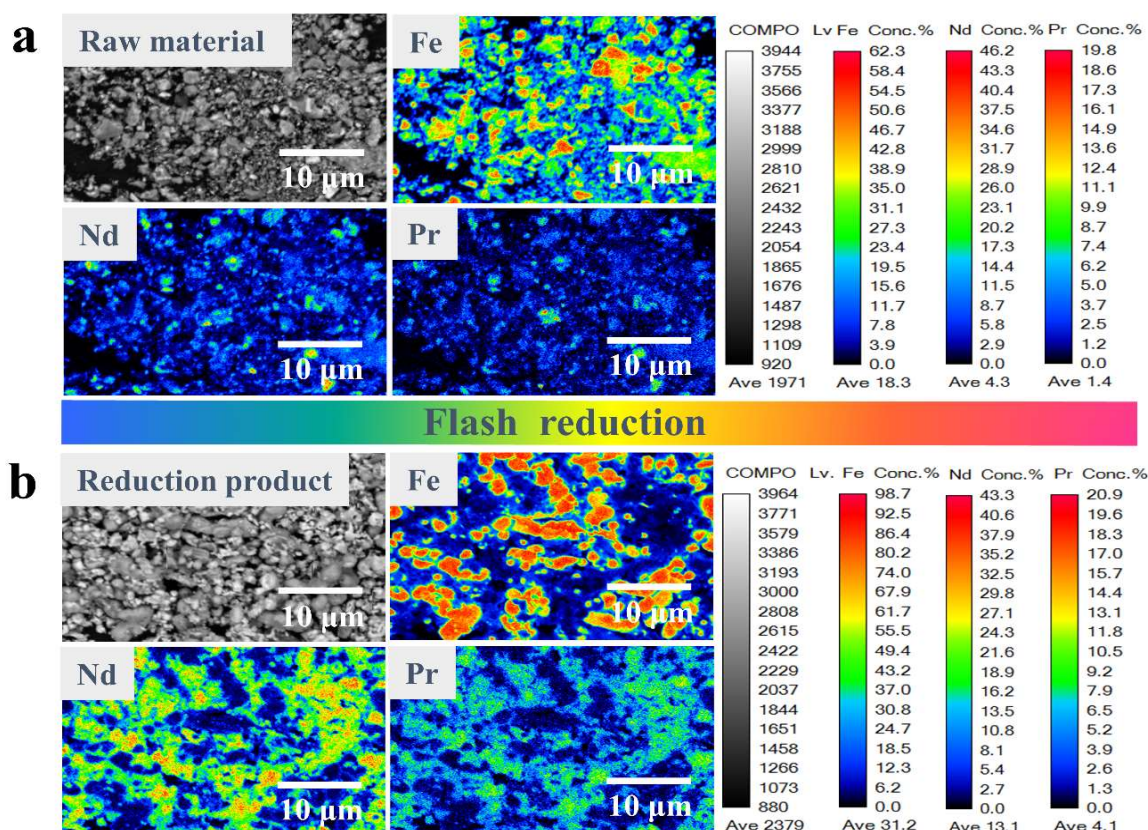


Figure 6. EPMA analysis of the product (a) before and (b) after flash reduction.

The comparison and analysis of technological conditions for reducing Fe_2O_3 from hematite or NdFeB scrap to metallic Fe, as presented in Table 3 [26–30], yield several significant findings. Firstly, the conventional reduction method necessitates a lengthy reaction time that typically exceeds one hour. In contrast, the flash reduction method stands out by significantly reducing this reaction time, optimizing efficiency. Secondly, the gas–solid reduction process exhibits a notably faster reaction rate when compared to the solid–solid reduction process. Moreover, it manages to achieve this accelerated reaction rate while also lowering the required reaction temperature. This result highlights the advantages of the gas–solid reduction approach in terms of both speed and energy efficiency. Thirdly, it is observed that the reduction temperature decreases as the particle size of a raw material becomes finer. Leveraging this characteristic, the flash reduction method, conducted under a hydrogen atmosphere, successfully capitalizes on the small particle size of the raw materials. This strategic choice has led to a substantial reduction in both reaction temperature and duration, marking a significant advancement in the reduction process’s efficiency and sustainability.

Table 3. Comparison for reducing Fe_2O_3 from hematite or NdFeB scrape to metallic Fe.

Ref.	Method	Reductant	Particle Size	T/K	Time	Reduction Rate/%
[26]	Gas–solid reduction	$\text{H}_2 + \text{CO}$	~150 μm	1373	60 min	94.7
[27]	Flash reduction	$\text{H}_2 + \text{CO}$	21 μm	1623	5 s	90
[28]	Solid–solid reduction	C	74 μm	1473	240 min	88.08
[29]	Solid–solid reduction	C	150 μm	1823	60 min	99.12
[30]	Solid–solid reduction	C	~100 μm	1773	240 min	99.8
This work	Flash reduction	H_2	0.45 μm	723	5 s	95.2

3.4. Effect of Magnetic Field Intensity on the Separation Rate of Fe/REOs

Based on the magnetic differences between the reduction products, Fe and REOs were separated using a magnetic tube [31,32]. The effect of magnetic separation field intensity on the separation rate was initially investigated. The yield of Fe powder increased with the increasing magnetic field intensity, and the presence of REOs in the Fe-rich phase simultaneously increased. When the magnetic field intensity increased to 240 mT, a maximum yield of Fe (~80%) was attained (Figure 7a); however, the content of REOs retained in the Fe-rich phase approached 16 wt% (Figure 7b), resulting in a decrease in Fe content in Fe-rich phase (Figure 7c). One-step magnetic separation would result in a significant waste of REOs. Therefore, a weak field intensity is used for the second-stage magnetic separation of the Fe-rich phase. Although the weaker magnetic separation decreases the Fe yield (82.8 to 54.7%), the REOs can be effectively recovered. Particularly, when the magnetic separation intensity is 40 mT, the yield of Fe reaches 54.7% (Figure 7d), the content of REOs in the Fe-rich phase decreases from ~16 to 4.1 wt% (Figure 7e), and the content of Fe in the Fe-rich phase is enriched from ~80 to 90.2% (Figure 7f). Therefore, the proposed two-stage magnetic separation is suitable for separating Fe- and REO-rich phases.

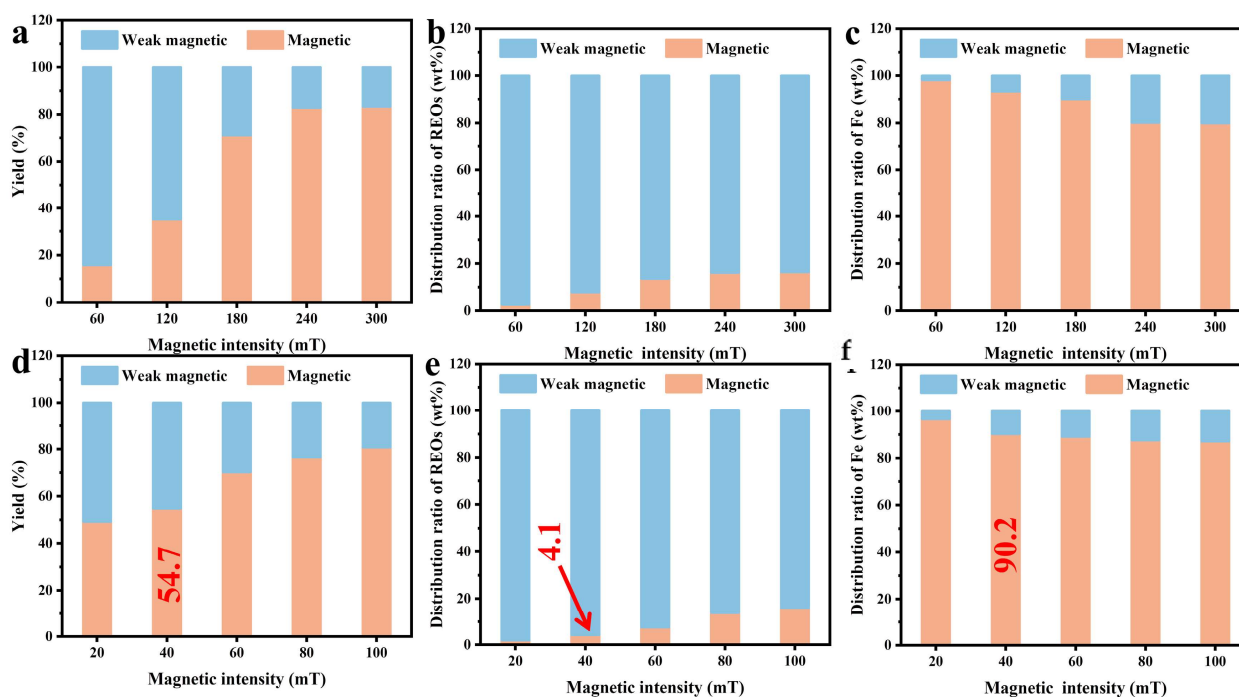


Figure 7. Effect of magnetic field intensity on separation rate of Fe/REOs: yield of first-step magnetic separation; (a) distribution ratio of REOs (b) and Fe (c) in first-step magnetic separation; yield of second-step magnetic separation; (d) distribution ratio of REOs (e) and Fe (f) in second-step magnetic separation.

To further verify the effectiveness of the two-stage magnetic separation process, magnetic separation products (Fe- and REO-rich phases) were characterized using XRD (Figure 8) and EPMA (Figure 9). The primary component of the Fe-rich phase is metallic Fe (PDF# 03-065-4899), with small amounts of SiO₂ (PDF# 01-083-2469) and Nd₂O₃ (PDF# 01-028-0671). This is the case owing to the small particle size of the sample with weak magnetic field intensity carried by metallic Fe. The REO-rich phase, with its poor crystal form, predominantly contains SiO₂ and Nd₂O₃, which can be ascribed to the formation of glassy slag in the reduction process [33,34].

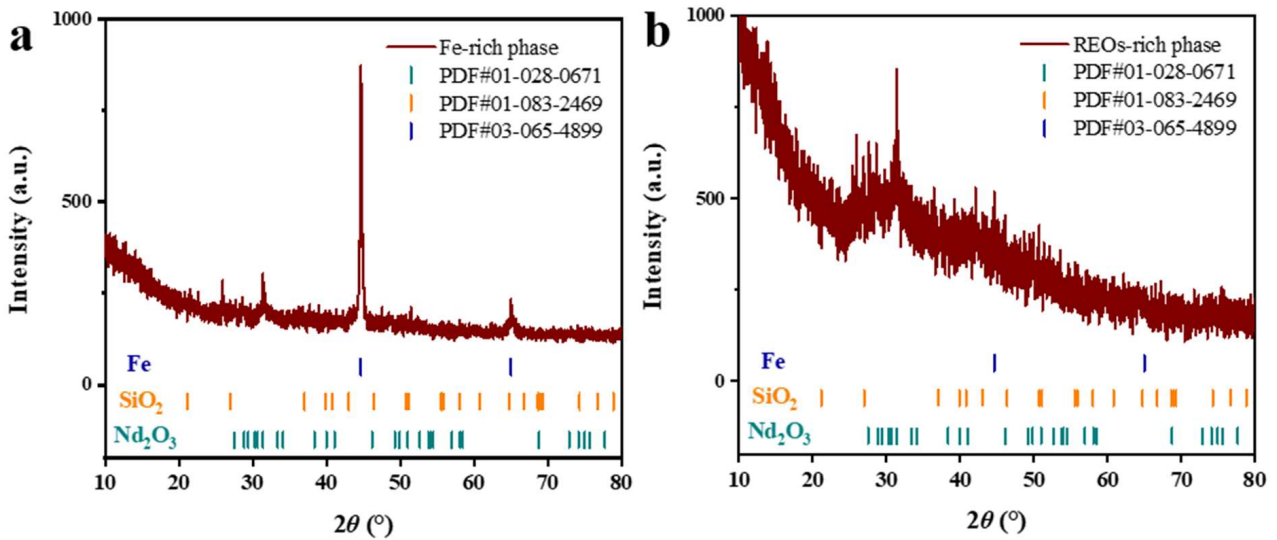


Figure 8. XRD patterns of the Fe-rich phase (a) and REOs-rich phase (b).

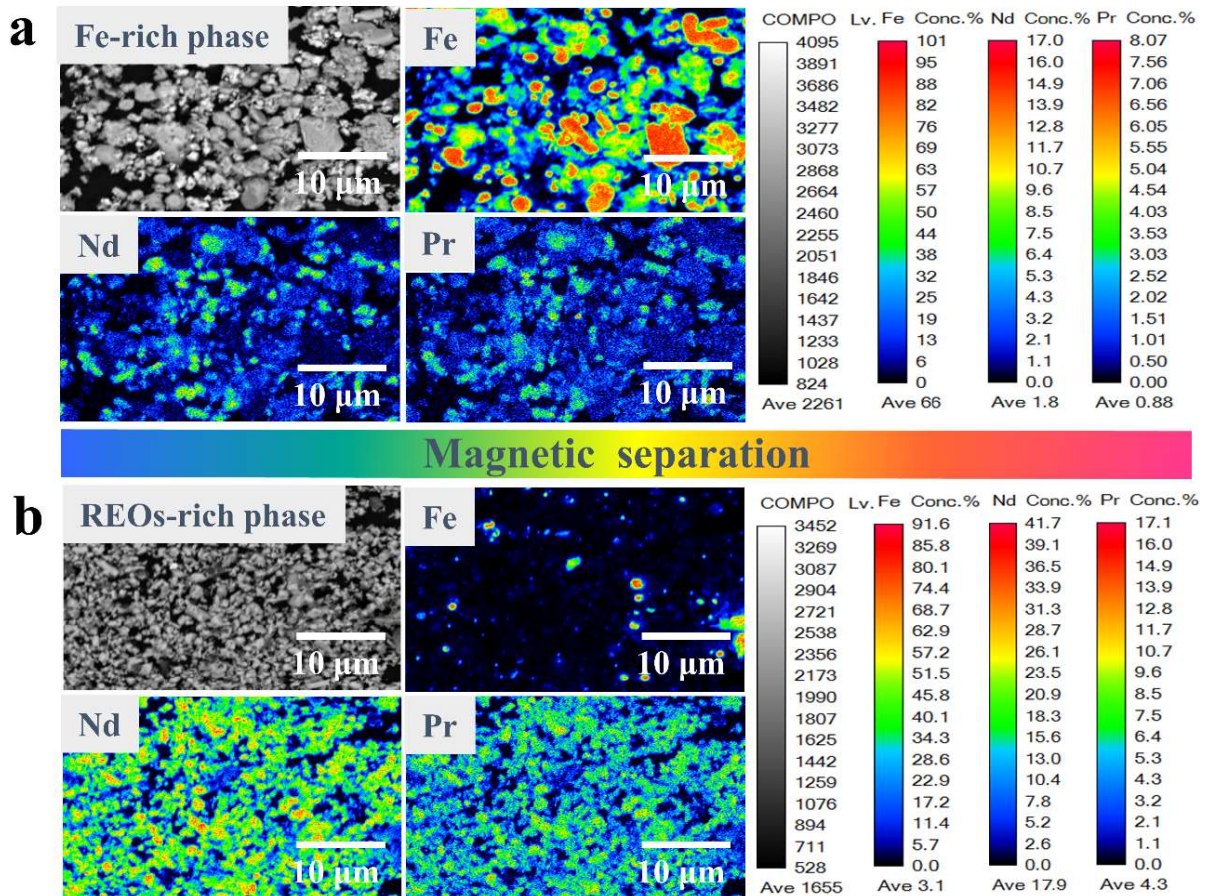


Figure 9. EPMA analysis of the product by magnetic separation: (a) Fe-rich phase, (b) REOs-rich phase.

The morphological results indicate that the particle size of the Fe-rich phase is larger than that of the REO-rich phase. Additionally, its morphology is consistent with that of the reduced product (Figure 9). The mapping results in Figure 9 verify the favorable effect of the two-stage magnetic separation. Fe and REOs are successfully separated via magnetic separation. The REO-rich phase is recovered using the conventional hydrochloric acid method [35,36]. The process used in this study significantly minimizes the interference of

Fe in NdFeB magnet scraps with the leaching of REOs, and the burden of subsequent Fe purification is decreased.

Meanwhile, ICP was utilized to further analyze the quantitative components of the Fe-rich and REOs-rich phases, and the results are presented in Table 4. The findings revealed that the Fe content in the NdFeB calcine increased from 45.9 wt% to 55.6 wt% after flash reduction, while the REOs content in the NdFeB calcine increased from 30.2 wt% to 36.8 wt% following flash reduction. Although a one-step magnetic separation process yielded a high quantity of strong magnetic material, the Fe-rich phase only contained 65.2 wt% of Fe, while the REOs content reached as high as 29.1 wt%, resulting in a significant loss of REOs. However, in the second step of magnetic separation, the yield of the Fe-rich phase was only 67.2%. Nevertheless, the content of Fe in the strong magnetic material increased from 65.2 wt% to 90.2 wt%, and the REOs content in the Fe-rich phase decreased from 29.1 wt% to 3.1 wt%. Conversely, the REOs content in the REOs-rich phase of the low magnetic separation material increased from 30.2 wt% to 82.8 wt%, while the Fe content in the REOs-rich phase decreased from 45.9 wt% to 13.5 wt%. Consequently, after separating Fe/REOs in the NdFeB calcine through the flash reduction–magnetic separation process, the following benefits are observed: (1) The utilization efficiency of a significant amount of iron in NdFeB scraps is significantly improved and can be directly utilized as raw material for iron production. (2) The acid consumption required to dissolve calcine is reduced, and the concentration of rare earth in the leaching solution is increased. (3) The generation of a substantial quantity of leaching waste residue rich in rare earth phases is avoided.

Furthermore, the mass balance of REOs and Fe during flash reduction–magnetic separation is calculated and analyzed (Figure 10). The flash reduction experiment used 100 g of the raw material as its basis. According to the reduction rate of Fe (95.2%) under the optimal reduction conditions, the mass of the reduced product is 80.3 g. Magnetic separation is used to obtain REOs and Fe. In the first magnetic separation step, although the Fe-rich phase is recovered with a 82.8% yield, the resulting loss of REOs is 16.1 wt%. Therefore, the use of weak magnetic separation is proposed. Although the Fe-rich phase yield is only 54.7%, the Fe and REO distribution rates in the Fe- and REO-rich phases reach 90.2 and 95.9%, respectively. Therefore, metallic Fe can be effectively separated and REOs can be significantly enriched using this method.

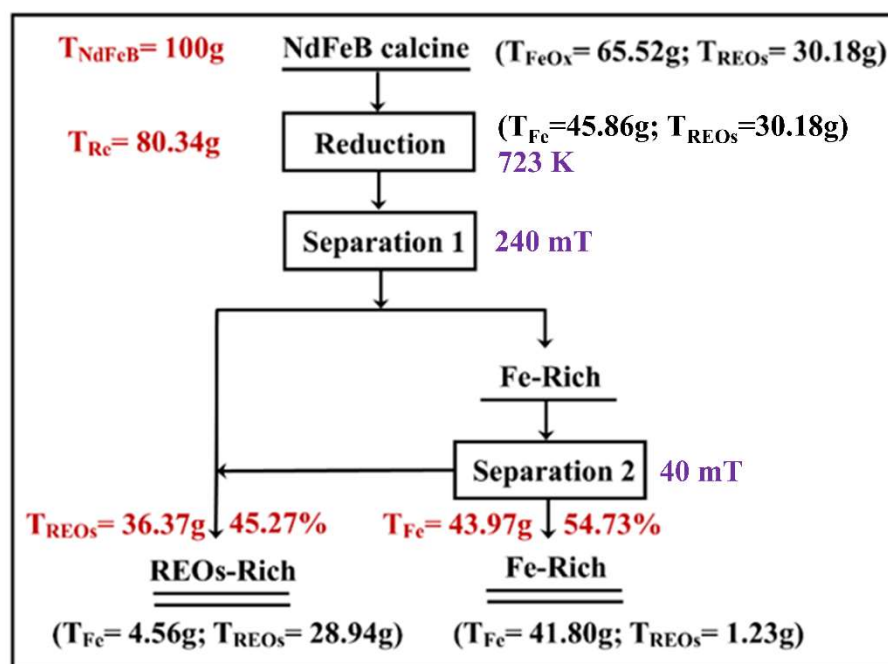


Figure 10. Mass balance of the NdFeB calcine in flash reduction-magnetic separation process.

Table 4. Chemical composition of the calcined NdFeB, reduction product, Fe-rich and REOs-rich phases.

Composition		Fe wt%	REOs wt%	Yield %
calcined NdFeB		45.9	30.2	/
Reduction product		55.6	36.8	/
First step separation	Fe-rich phase	65.2	29.1	82.8
	REOs-rich phase	9.5	74.0	17.2
Second step separation	Fe-rich phase	90.2	3.1	67.4
	REOs-rich phase	13.5	82.8	32.6

4. Conclusions

A method involving flash reduction and magnetic separation was developed to effectively separate Fe and enrich REOs from NdFeB magnet scraps. Initially, the feasibility of selectively reducing FeO_x was predicted using thermodynamic analysis. The optimization of reduction conditions showed that increasing the reaction temperature and reducing the particle size enhanced the reduction rate of Fe significantly. Ultimately, the reduction rate of FeO_x surpassed 95% under optimal conditions (temperature 723 K, D₉₀ = 0.45 μm, H₂ flow rate 2.0 L/min) due to efficient mass and heat transfer, which facilitated the reduction kinetics. This conclusion was further supported by XRD and EPMA analysis, confirming the selective reduction of FeO_x. Next, the process proceeded to separate metallic Fe and REOs from the reduction product through magnetic separation. Initially, a one-step magnet separation process was tested, employing a magnetic field intensity of 240 mT. Although this achieved a Fe yield of 82.8% with a distribution ratio of 80.1 wt% and a high REO distribution ratio of 16.1 wt% in the Fe-rich phase, a significant quantity of rare earths was wasted in this approach. To mitigate the loss of valuable rare earths, a two-step magnet separation process was implemented, utilizing a magnetic field intensity of 40 mT. Despite the reduction in Fe yield to 67.4%, this modification led to a remarkable increase in the distribution ratio of Fe to 90.2 wt%, while the distribution ratio of REOs decreased to 4.1 wt%. Consequently, these Fe-rich phases could be utilized as inexpensive raw materials in weathering steel production without necessitating additional pretreatments. Flash reduction and magnetic separation process not only exhibit the advantages of having a short process and low energy consumption, but they also realize the stepwise recovery of rare earth and Fe.

Author Contributions: Conceptualization, H.W. and J.W.; methodology, X.W.; software, S.X.; validation, X.L., D.L. and F.L.; formal analysis, W.Z.; investigation, H.W.; resources, J.W.; data curation, H.W.; writing—original draft preparation, H.W.; writing—review and editing, S.X.; supervision, J.W.; project administration, J.W.; funding acquisition, J.W. All authors have read and agreed to the published version of the manuscript.

Funding: This work was financially supported by the China Baowu Low Carbon Metallurgy Innovation Foundation (BWLCF202121), the Jiangxi Provincial Key Laboratory of Flash Green Development and Recycling (20193BCD40019), Academic and technical leaders of major disciplines in Jiangxi Province (20213BCJ22003), and Jiangxi Province Science and Technology innovation talent project (jxsq2023201012).

Data Availability Statement: All relevant data are within the paper.

Conflicts of Interest: The authors declare no competing interest.

References

- Dudarko, O.; Kobylinska, N.; Kessler, V.; Seisenbaieva, G. Recovery of rare earth elements from NdFeB magnet by mono- and bifunctional mesoporous silica: Waste recycling strategies and perspectives. *Hydrometallurgy* **2022**, *2022*, 105855. [[CrossRef](#)]
- Laatikainen, M.; Makarova, I.; Sainio, T.; Repo, E. Selective acid leaching of rare earth elements from roasted NdFeB magnets. *Sep. Purif. Technol.* **2021**, *278*, 119571. [[CrossRef](#)]

3. Klemettinen, A.; Zak, A.; Chojnacka, I.; Matuska, S.; Le'sniewicz, A.; Wehna, M.; Adamski, Z.; Klemettinen, L.; Rycerz, L. Leaching of Rare Earth Elements from NdFeB Magnets without Mechanical Pretreatment by Sulfuric (H_2SO_4) and Hydrochloric (HCl) Acids. *Minerals* **2021**, *11*, 1374. [[CrossRef](#)]
4. Bohm, D.; Czerski, K.; Gottlieb, S.; Huke, A.; Ruprecht, G. Recovery of Rare Earth Elements from NdFeB Magnets by Chlorination and Distillation. *Processes* **2023**, *11*, 577. [[CrossRef](#)]
5. München, D.D.; Stein, R.T.; Veit, H.M. Rare Earth Elements Recycling Potential Estimate Based on End-of-Life NdFeB Permanent Magnets from Mobile Phones and Hard Disk Drives in Brazil. *Minerals* **2021**, *11*, 1190. [[CrossRef](#)]
6. Habibzadeh, A.; Ali Kucuker, M.; Gokelma, M. Review on the Parameters of Recycling NdFeB Magnets via a Hydrogenation Process. *ACS Omega* **2023**, *8*, 17431–17445. [[CrossRef](#)]
7. Saito, T.; Sato, H.; Ozawa, S.; Yu, J.; Motegi, T. The extraction of Nd from waste NdFeB alloys by the glass slag method. *J. Alloys Compd.* **2003**, *353*, 189–193. [[CrossRef](#)]
8. Mochizuki, Y.; Tsubouchi, N.; Sugawara, K. Selective Recovery of Rare Earth Elements from Dy containing NdFeB Magnets by Chlorination. *ACS Sustain. Chem. Eng.* **2013**, *1*, 655–662. [[CrossRef](#)]
9. Sun, M.; Hu, X.Y.; Peng, L.M.; Fu, P.H.; Ding, W.J.; Peng, Y.H. On the production of Mg-Nd master alloy from NdFeB magnet scraps. *J. Mater. Process. Technol.* **2015**, *218*, 57–61. [[CrossRef](#)]
10. Kumari, A.; Randhawa, N.S.; Sahu, S.K. Electrochemical treatment of spent NdFeB magnet in organic acid for recovery of rare earths and other metal values. *J. Clean. Prod.* **2021**, *309*, 127393. [[CrossRef](#)]
11. Brahim, J.A.; Hak, S.A.; Achiou, B.; Boulif, R.; Beniazza, R.; Benhida, R. Kinetics and mechanisms of leaching of rare earth elements from secondary resources. *Miner. Eng.* **2022**, *177*, 107351. [[CrossRef](#)]
12. Makarava, I.; Kasach, A.; Kharytonau, D.; Kurilo, I.; Laatikainen, M.; Repo, E. Enhanced acid leaching of rare earths from NdCeFeB magnets. *Miner. Eng.* **2022**, *179*, 107446. [[CrossRef](#)]
13. Ding, J.; Li, Y.; Yong, P.T. A comparative study of melt-spun ribbons of $Nd_{12}Fe_{82}B_6$ and $Nd_{15}Fe_{77}B_8$. *J. Phys. D Appl. Phys.* **1998**, *31*, 2745. [[CrossRef](#)]
14. Ling, Z.Y.; Xiong, M.R.; Zhang, Q.Q. Effects of iron deficiency on magnetic properties of $(Ni_{0.76}Zn_{0.24})O(Fe_2O_3)_{0.575}$ ferrite. *J. Magn. Magn. Mater.* **2000**, *219*, 9–14. [[CrossRef](#)]
15. Tang, Z.D.; Zhang, Q.; Sun, Y.S.; Gao, P.; Han, Y.X. Pilot-scale extraction of iron from flotation tailings via suspension magnetization roasting in a mixture of CO and H_2 followed by magnetic separation. *Resour. Conserv. Recycl.* **2021**, *172*, 105680. [[CrossRef](#)]
16. Pineau, A.; Kanari, N.; Gaballah, I. Kinetics of reduction of iron oxides by H_2 : Part I: Low temperature reduction of hematite. *Thermochim. Acta* **2006**, *447*, 89–100. [[CrossRef](#)]
17. Pineau, A.; Kanari, N.; Gaballah, I. Kinetics of reduction of iron oxides by H_2 : Part II. Low temperature reduction of magnetite. *Thermochim. Acta* **2007**, *456*, 75–88. [[CrossRef](#)]
18. Wang, J.L.; Peng, R.Z. Flash Reduction Comprehensive Recovery Method of Neodymium Iron Boron Waste Acid Leaching Residue. CN201910009569.7, 4 January 2019.
19. Wang, J.L.; Wang, H.Q. A Method for One-Step Comprehensive Recovery of NdFeB Waste Acid Leaching Slag by Flash Reduction. CN201910009567.8, 4 January 2019.
20. Zhang, H.B.; Wang, Y.N.; He, Y.Z.; Xu, S.H.; Hu, B.; Cao, H.Z.; Zhou, J.; Zheng, G.Q. Efficient and safe disposition of arsenic by incorporation in smelting slag through copper flash smelting process. *Miner. Eng.* **2021**, *160*, 106661. [[CrossRef](#)]
21. Bao, Q.P.; Guo, L.; Guo, Z.C. A novel direct reduction-flash smelting separation process of treating high phosphorous iron ore fines. *Power Technol.* **2021**, *377*, 149–162. [[CrossRef](#)]
22. Constantineau, J.P.; Bouffard, S.C.; Grace, J.R.; Richards, G.G. Pre-ignition behavior of lead sulfide in the flame of a flash smelter. *Miner. Eng.* **2011**, *24*, 845–851. [[CrossRef](#)]
23. Speight, J. *Lange's Handbook of Chemistry*; McGraw-Hill Education: Columbus, OH, USA, 2005.
24. Pang, J.M.; Guo, P.M.; Zhao, P.; Cao, C.Z.; Zhang, D.W. Influence of Size of Hematite Powder on Its Reduction Kinetics by H_2 at Low Temperature. *J. Iron Steel Res. Int.* **2009**, *16*, 7–11. [[CrossRef](#)]
25. Jozwiak, W.K.; Kaczmarek, E.; Maniecki, T.P.; Ignaczak, W.; Maniukiewicz, W. Reduction behavior of iron oxides in hydrogen and carbon monoxide atmospheres. *Appl. Catal. A Gen.* **2007**, *326*, 17–27. [[CrossRef](#)]
26. Stopic, S.; Polat, B.; Chung, H.W.; Emil-Kaya, E.; Smiljanic, S.; Gurmen, S.; Friedrich, B. Recovery of Rare Earth Elements through Spent NdFeB Magnet Oxidation (First Part). *Metals* **2022**, *12*, 1464. [[CrossRef](#)]
27. Luo, S.Y.; Yi, C.J.; Zhou, Y.M. Direct reduction of mixed biomass- Fe_2O_3 briquettes using biomass-generated syngas. *Renew. Energy* **2011**, *36*, 3332–3336. [[CrossRef](#)]
28. Chen, F.; Mohassab, Y.; Zhang, S.Q.; Sohn, H.Y. Kinetics of the Reduction of Hematite Concentrate Particles by Carbon Monoxide Relevant to a Novel Flash Ironmaking Process. *Metall. Mater. Trans. B* **2015**, *46*, 1716–1728. [[CrossRef](#)]
29. Wang, J.L.; Liu, X.R. Carbon-Thermal Reduction of Neodymium Iron Boron Scrap. *J. Chin. Soc. Rare Earths* **2020**, *37*, 84–90. [[CrossRef](#)]
30. Bang, Y.Y.; Guo, S.Q.; Xu, Y.L.; Tang, K.; Lu, X.G.; Ding, W.Z. Recovery of rare earth elements from permanent magnet scraps by pyrometallurgical process. *Rare Met.* **2022**, *41*, 1697–1702. [[CrossRef](#)]
31. Bang, Y.Y.; Guo, S.Q.; Tang, K.; Jiang, L.; Lu, C.Y.; Lu, X.G.; Ding, W.Z. Recovery of Rare Earth Elements from NdFeB Magnet Scraps by Pyrometallurgical Processes. In *Rare Metal Technology*; Springer: Cham, Switzerland, 2015. [[CrossRef](#)]

32. Yu, J.W.; Li, Y.F.; Lv, Y.; Han, Y.X.; Gao, P. Recovery of iron from high-iron red mud using suspension magnetization roasting and magnetic separation. *Miner. Eng.* **2022**, *178*, 107394. [[CrossRef](#)]
33. Ozawa, S.; Sato, H.; Saito, T.; Motegi, T.; Yu, J. Production of Nd-Fe-B alloys by the glass slag method. *J. Appl. Phys.* **2002**, *10*, 8831–8833. [[CrossRef](#)]
34. Saito, T. Structures and magnetic properties of Nd–Fe alloys produced by the glass slag method. *J. Alloys Compd.* **2006**, *414*, 88–93. [[CrossRef](#)]
35. Kumari, A.; Kumar Sahu, S. A comprehensive review on recycling of critical raw materials from spent neodymium iron boron (NdFeB) magnet. *Sep. Purif. Technol.* **2023**, *317*, 123527. [[CrossRef](#)]
36. Kumari, A.; Kumar Sinha, M.; Pramanik, S.; Kumar Sahu, S. Recovery of rare earths from spent NdFeB magnets of wind turbine: Leaching and kinetic aspects. *Waste Manag.* **2018**, *75*, 486–498. [[CrossRef](#)] [[PubMed](#)]

Disclaimer/Publisher’s Note: The statements, opinions and data contained in all publications are solely those of the individual author(s) and contributor(s) and not of MDPI and/or the editor(s). MDPI and/or the editor(s) disclaim responsibility for any injury to people or property resulting from any ideas, methods, instructions or products referred to in the content.